23 August 2004
Paper prepared for publication in TMS' JOM (Journal of Metals) in January 2005

# Comparison of Electrochemical Methods to Determine Crevice Corrosion Repassivation Potential of Alloy 22 in Chloride Solutions

Kenneth J. Evans, Ahmet Yilmaz, S. Daniel Day, Lana L. Wong, John C. Estill and Raúl B. Rebak

Lawrence Livermore National Laboratory, Livermore, CA 94550

## ABSTRACT

Alloy 22 (N06022) is a nickel-based alloy highly resistant to corrosion. In some aggressive conditions of high chloride concentration, temperature and applied potential, Alloy 22 may suffer crevice corrosion, a form of localized corrosion. There are several electrochemical methods that can be used to determine localized corrosion in metallic alloys. One of the most popular for rapid screening is the cyclic potentiodynamic polarization (CPP). This work compares the repassivation potentials obtained using CPP to related repassivation potential values obtained using the Tsujikawa-Hisamatsu Electrochemical (THE) method and the potentiostatic (POT) method. Studied variables included temperature and chloride concentration. The temperature was varied from 30°C and 120°C and the chloride concentration was varied between 0.0005 M to 4 M. Results show that similar repassivation potentials were obtained for Alloy 22 using CPP and THE methods. Generally, under more aggressive conditions, the repassivation potentials were more conservative using the CPP method. POT tests confirmed the validity of the repassivation potential as a threshold below which localized corrosion does not nucleate. The mode of attack in the tested specimens varied depending if the test method was CPP or THE; however, the repassivation potential remained the same.

## INTRODUCTION

Many austenitic alloys such as Alloy 22 (N06022) that rely on the stability of a thin chromium oxide ($Cr_2O_3$) film for protection against corrosion are prone to crevice corrosion, a form of localized corrosion. Localized corrosion is an insidious type of attack, which forms at discrete sites of the component surface and has a larger propagation rate than passive corrosion. Both ASTM and NACE International define crevice corrosion as "localized corrosion of a metal surface at, or immediately adjacent



to, an area that is shielded from full exposure to the environment because of close proximity between the metal and the surface of another material" [1]

The susceptibility of each individual alloy to localized corrosion depends strongly on the composition of the electrolyte solution, temperature and applied potential. In general, the environment becomes more aggressive with increases in chloride concentration, temperature and applied potential. Not all alloys that rely on a chromium oxide film for protection against corrosion have the same susceptibility to localized corrosion promoted by chloride. Alloys containing increased amount of chromium, molybdenum and nitrogen exhibit superior resistance to this type of attack. Thus, nickel-based Alloy 22 (N06022) has a greater resistance, for example, to crevice corrosion than iron-based type 316 stainless steel (S31600) since N06022 contains 22% chromium (Cr) and 13% molybdenum (Mo) and S31600 contains 18% Cr and 2.5% Mo.

Alloy 22 or N06022 is nickel-based (Ni) and contains by weight 22% chromium (Cr), 13% molybdenum (Mo), 3% tungsten (W) and approximately 3% iron (Fe). Alloy 22 was commercially designed to resist the most aggressive industrial applications, offering a low general corrosion rate both under oxidizing and reducing conditions [2]. Under oxidizing and acidic conditions Cr exerts its beneficial effect in the alloy. Under reducing conditions the most beneficial alloying elements are Mo and W, which offer a low exchange current for hydrogen discharge [3,4]. Moreover, due to its balanced content in Cr, Mo and W, Alloy 22 is used extensively in hot chloride containing environments where austenitic stainless steels may fail by pitting corrosion and stress corrosion cracking (SCC) [3,4].

Alloy 22 was selected for the fabrication of the outer shell of the high level nuclear waste containers for the proposed Yucca Mountain repository [5,6]. Several papers have been published recently describing the general and localized corrosion resistance of Alloy 22 regarding its application for the nuclear waste containers [6-17]. The Cyclic Potentiodynamic Polarization (CPP) (ASTM G 61) [1] was a popular method used to assess the anodic behavior of Alloy 22 and its response to localized corrosion. Other methods that were used to investigate localized corrosion included variations of the technique originally proposed by Tsujikawa and Hisamatsu [18] and later used by other researchers for different alloys [12,19,20]. It has been recently reported that the repassivation potential (ER) for Alloy 22 in 1 M NaCl and 5 M $CaCl_2$ at 90°C measured

using CPP and THE were similar [20]. For these two solutions, the ER values from CPP were slightly lower (more conservative) than the values from THE [20].

It is known that the presence of nitrate inhibits the nucleation and propagation of localized corrosion (crevice corrosion) in Alloy 22 [7-14,16-17]. It was reported that it is necessary to have a minimum ratio of $[NO_3^-]/[Cl^-]$ in the order of 0.2 to 0.5 for the inhibition to be complete [12,16]. The inhibitive effect of nitrate ions will be discussed fully in another publication and it is not part of this work.

The objective of this research work was to investigate the localized corrosion behavior of Alloy 22 as a function of chloride concentration and temperature using three electrochemical methods, namely, the cyclic potentiodynamic polarization (CPP –ASTM G 61), the Tsujikawa-Hisamatsu Electrochemical (THE) method and the potentiostatic (POT) methods and to compare the obtained results. The results in this paper are for comparing testing methods only. A solution containing just chloride anions is not representative of a Yucca Mountain environment.

## EXPERIMENTAL

Alloy 22 specimens were mainly prepared from 1-inch thick plate. There were several heats of material used in this research. The chemical composition of the most used specimens of Alloy 22 are given in Table 1. The specimens were mainly multiple crevice assemblies (MCA), which were fabricated based on the washer for crevice forming described in ASTM G 48 and G 78 [1]. The MCA specimen has been described before [7,9]. Other specimens included the PCA or prism crevice assembly (Figure 1). The tested surface area of the MCA specimens was approximately 11 $cm^2$ and for the PCA 14 $cm^2$. Both MCA and PCA had the same crevicing mechanism. All the tested specimens had a finished grinding of abrasive paper number 600 and were degreased in acetone and treated ultrasonically for 5 minutes in de-ionized (DI) water 1 hour prior to testing. Specimens were used in the mill annealed (MA) and in the as-welded (ASW) condition. All of the specimens listed in Tables 3 and 4 were in the MA condition except for the ones with the designation JE and KE, which contained a weld seam. The weld was produced with matching filler metal using Gas Tungsten Arc Welding (GTAW). The welded specimens were not all weld metal but contained a weld seam which varied in



width from approximately 8 to15 mm. The weld seam run across the surface of the specimen that was purposely creviced with the multiple teeth washer (Figure 1).

Electrochemical tests were carried out in deaerated 0.0005 M to 1 M NaCl at 90°C and in 5 M $CaCl_2$ solutions from 30°C to 120°C. The pH of the NaCl solutions was approximately 5 to 6 and the $CaCl_2$ solution was approximately 4 to 5. Nitrogen ($N_2$) was purged through the solution at a flow rate of 100cc/min for 24 hours while the corrosion potential ($E_{corr}$) was monitored. Nitrogen bubbling was continued throughout all the electrochemical tests. The electrochemical tests were conducted in a one-liter, three-electrode, borosilicate glass flask (ASTM G 5) [1]. A water-cooled condenser combined with a water trap was used to avoid evaporation of the solution and to prevent the ingress of air (oxygen). The temperature of the solution was controlled by immersing the cell in a thermostatisized silicone oil bath. All the tests were carried out at ambient pressure. The reference electrode was saturated silver chloride (SSC) electrode, which at ambient temperature has a potential of 199 mV more positive than the standard hydrogen electrode (SHE). The reference electrode was connected to the solution through a water-jacketed Luggin probe so that the electrode was maintained at near ambient temperature. The counter electrode was a flag (36 $cm^2$) of platinum foil spot-welded to a platinum wire. All the potentials in this paper are reported in the SSC scale.

Basically the test sequence for each specimen consisted of three parts: (1) $E_{corr}$ evolution as a function of time for 24 h, (2) Polarization Resistance (ASTM G 59) three subsequent times and (3) A larger anodic polarization to determine susceptibility to crevice corrosion. The larger anodic polarization was conducted using three methods: (i) Cyclic Potentiodynamic Polarization (CPP) method, (ii) Tsujikawa-Hisamatsu Electrochemical (THE) method and (iii) Potentiostatic (POT) method. Only the results from the last three methods are reported in this paper.

**Cyclic Potentiodynamic Polarization - CPP (ASTM G 61)**: One of the tests to assess the susceptibility of Alloy 22 to localized corrosion and passive stability was the cyclic potentiodynamic polarization technique, CPP (ASTM G 61) [1]. The potential scan was started 150 mV below $E_{corr}$ at a set scan rate of 0.167 mV/s. The scan direction was reversed when the current density reached 5 $mA/cm^2$ in the forward scan. Depending on the range of applied potentials, each CPP test could last between 1 h and 3 h. This is a fast and efficient method to determine crevice corrosion parameters, such as the

repassivation potential cross over (ERCO) or the repassivation potential for which the overall current density is 1 μA/cm² (ER1).

**Tsujikawa-Hisamatsu Electrochemical - THE**: The second test used to assess the susceptibility of Alloy 22 to localized corrosion and passive stability was the Tsujikawa-Hisamatsu Electrochemical test, which still does not have a ASTM standard even though it was introduced to the corrosion community about 20 years ago [18]. The potential scan was started 150 mV below $E_{corr}$ at a set potentiodynamic scan rate of 0.167 mV/s. Once the current density reached a predetermined value (for example 20 μA/cm² or 2 μA/cm²), the controlling mode was switched from potentiodynamic to galvanostatic and the predetermined current density is applied for usually 2 h. Some tests were conducted holding a galvanostatic treatment for 4 h and 8 h. The resulting potential at the end of the galvanostatic treatment was recorded. After the galvanostatic step, the treatment was switched to a potentiostatic mode. The potentiostatic steps were applied for 2 h starting at the potential recorded at the end of the galvanostatic treatment and applying as many steps as necessary until crevice repassivation was achieved. Each subsequent potentiostatic step was 10 mV lower that the previous step. Generally 10 steps (or a total of 100 mV) were necessary to achieve repassivation of an active crevice-corrosion. The repassivation potential is determined as the potential for which the current density decreases as a function of time in the period of treatment of 2 h. Depending of the applied time and number of potentiostatic steps, each THE test could last between 24 h and 30 h. This is a lengthy test, which yields only one parameter, the crevice repassivation potential (ER, CREV). The determination of ER,CREV may me subjective.

**Potentiostatic Tests - POT**: The third method is the potentiostatic test, which does not have a specific ASTM standard developed for it. After the repassivation potential is obtained using either CPP or THE a potential just below ER or just above ER is selected and applied to a creviced specimen while the output current is recorded as a function of time. If the current increases, it is assumed that crevice corrosion initiated and propagated. If the current density decreased as a function of time it is assumed that the specimen remained passive.

After the CPP, THE and POT tests, the specimens were examined in an optical stereomicroscope at a magnification of 20 times to establish the mode and location of the attack. A few specimens were also studied using a scanning electron microscope (SEM).



## RESULTS AND DISCUSSION

The comparison of the electrochemical techniques will be carried out in two separate sections. In the first part the localized corrosion behavior of Alloy 22 is studied as a function of the temperature from 30°C to 120°C in 5 M $CaCl_2$ solution. In the second part, the effect of chloride concentration (as NaCl) at a fixed temperature of 90°C is studied. The chloride concentration was varied from 0.0005 M to 4 M.

### The Effect of Temperature

Cyclic Potentiodynamic Polarizations (CPP)

In the cyclic potentiodynamic polarization (CPP) curves (e.g. Figure 2) there are several typical potentials. One of these potentials is the corrosion potential or the potential for which the applied cathodic and anodic currents are the same. The passive current density is defined as the region of potentials in which the current density is not highly dependent on the applied potential. Another typical potential is the breakdown potential for which the current density increases significantly and rather rapidly above the passive current density. In this paper we define breakdown potential as E20 or the potential that the specimen needs to reach to carry a current density of 20 μA/cm². The repassivation potential is the potential for which the specimen regains current behaviors typical of pre-breakdown values. In this paper we use two different repassivation potentials. One is ER1 or the potential for the specimen to reach 1 μA/cm² in the reverse scan. The second repassivation potential is ERCO or the potential for which the forward and reverse scans intersect (Figure 2). Figure 2 shows arrows indicating the values of current density of 20 μA/cm² (E20) for the forward scan and 1 μA/cm² (ER1) for the reverse scan. The cross-over potential (ERCO) is also indicated in Figure 2.

Figure 2 shows the cyclic potentiodynamic polarization welded Alloy 22 specimens in deaerated 5 M $CaCl_2$ at 30°C and 90°C. The passive current density for the two specimens was practically the same and between 0.1 μA/cm² and 1 μA/cm². For the specimen tested at 90°C, the breakdown potential (E20) was 71 mV (SSC) and for the specimen tested at 30°C, the breakdown potential was 989 mV (SSC). At 90°C, Alloy 22 showed a classical passive region with the current density practically independent of applied potential until the breakdown potential. Then, the current density increased

abruptly and the reverse polarization showed a clear hysteresis, suggesting the nucleation and growth of localized corrosion at the point of potential breakdown. After the tests, the examined specimen showed that localized attack started at the crevice formers and progressed outwards towards the metal exposed boldly to the solution. The attack was related to the presence of the crevice former but did not propagate below the crevice former. This has been reported before [9,20]. The highest polarization for Alloy 22 at 90°C in Figure 2 was less than 0.2 V (SSC). The localized attack in welded specimens occurred equally in the base metal and in the weld seam. In many cases, the amount of localized corrosion attack was higher in the base material than in the weld material. The specimen polarized at 30°C had a typical anodic peak midway in the passive region (at +250 mV SSC) and then regained its passivity and eventually reached very high values of potential (1.2 V SSC). The reverse scan traced back the forward scan suggesting the absence of localized corrosion (Figure 2). After the test the specimen showed abundant transpassive behavior and weld etching due to the high applied potentials. The specimen was free from localized corrosion.

Parameters from Cyclic Potentiodynamic Polarization (CPP) Curves

Figure 3 shows values of ER1 and ERCO for as-welded (ASW) and mill annealed (MA) creviced specimens of Alloy 22 tested in 5 M $CaCl_2$ as a function of the temperature. Some of these data has been published before [9,10,20]. The repassivation potentials (ER1 and ERCO) decreased as the temperature increased. The drop in the repassivation potential was considerably (approx. 600 mV or 20 mV/°C) between 30°C and 60°C and then more gradually or ten times slower between 60°C and 120°C (less than 200 mV or 2 mV/°C). Using CPP, most specimens suffered localized corrosion at 60°C and higher temperatures and were generally free from localized corrosion at the lower temperatures. Figure 3 shows that the average values of ER1 and ERCO are similar to each other; therefore, in further comparisons of the methods only the value of ER1 is used. The value of ER1 is preferred here since it is always obtainable from a polarization curve, however the value of ERCO is only available when a cross over is evident. Figure 3 also shows that the difference in the repassivation potential between MA and ASW specimens is practically nil.



Tsujikawa Hisamatsu Electrochemical (THE)

Figures 4 shows the results from THE tests for an Alloy 22 MCA specimen in 5 M $CaCl_2$ at 30°C. The repassivation potentials (ER,CREV) is defined [18-20] as the potential for which the current does not increase as a function of time for a period of 2 h. For the test shown in Figure 4, ER,CREV is –4 mV SSC. Figure 5 shows that the tested specimen suffered crevice corrosion under the crevicing washer. The attack was in the form of grain boundary etching in the base metal and interdendritic dissolution in the weld metal. The attack was shallow. The average values of ER,CREV are listed in Table 2. Some of the individual results were reported before [20].

Comparison Between CPP and THE

Figure 6 compares the crevice repassivation potentials determined using CPP (ER1) and the ER,CREV obtained using THE tests. The values of ER1 and ER,CREV fully agree with each other in the intermediate range of temperature, that is, between approximately 60°C and 75°C. The values of repassivation potential ER,CREV are lower than ER1 at the lower temperatures (30°C-60°C) and higher at the higher temperatures (75°C-120°C). When using the CPP method at the lower temperatures (e.g. 30°C) the specimen is applied high potentials (currents) that causes transpassive dissolution in the boldly exposed surface and time is not allowed for the specimen to nucleate and propagate crevice corrosion since the CPP test lasts less than 3 h. That is, the transpassive dissolution may short circuit or overshadow any occurrence of crevice corrosion using CPP. In the short interval of 3 h, current densities as high as 5 mA/cm² were applied to the specimen causing abundant transpassivity. On the other hand, by using the THE test, a smaller amount of current density of only 2 μA/cm² is applied (Figure 4), which is used by the specimen mostly for nucleation and propagation of crevice corrosion. The total THE test lasted approximately 15 h, which seemed enough to propagate a shallow crevice attack (Figure 5). On the other hand, at the higher temperatures (e.g. 90°C), when using the CPP test, the potential is scanned fast to produce current densities in the order of 5 mA/cm² causing massive localized corrosion a the border between the crevice former and the specimen. When the specimen is polarized in reverse, potentials in the order of –180 mV SSC at 90°C (Table 2) are necessary to achieve to repassivate the specimen. Using the CPP method the localized attack is mostly outside the crevice former [20]. By using the THE test, a smaller amount of current density (approx. 25 μA/cm²) is used to

nucleate the crevice attack [20]. This produces attack only under the crevice formers that seem easier to repassivate since an applied potential of –130 mV SSC at 90°C is needed to cause repassivation (Table 2).

Constant Potential Tests (Potentiostatic or POT)

Table 2 shows that the repassivation potential of ASW Alloy 22 in 5 M $CaCl_2$ at 120°C is –215 mV SSC using the CPP test (ER1) and –136 mV SSC using the THE test (ER,CREV). A few potentiostatic tests (POT) were carried out to determine the crevice corrosion potential by applying a constant potential and monitoring the output current as a function of time. Figure 7 shows that specimens polarized at –200 mV and –150 mV did not suffer crevice corrosion as the current density decreased continuously as the time increased for the period of one week (168 h). The current density for the passivated specimens in Figure 7 was approximately one order of magnitude lower than the current density in the passive region of a CPP curve, even at the lower temperature of 90°C (Figure 2). The calculated dissolution rate for a current density of $5 \times 10^{-8}$ A/cm² (Figure 7) results is 0.4 μm/year. After the potentiostatic tests, the specimens did not show any discoloration or localized corrosion. On the other hand, the specimen polarized at –100 mV SSC suffered severe localized corrosion and the test was interrupted after two days of testing (Figure 7). The attack started at the crevice formers and propagated towards the outside, to the boldly exposed surface (Figure 8). The attack was typical crystalline due to the intergranular mode of attack of the base metal and interdendritic attack in the weld seam (Figure 8). Estimating that the area of attack for the specimen polarized at –100 mV (KE0154) was 15 percent (2 cm²) of the entire exposed surface of the specimen, the corrosion rate in the localized attack area was approximately 40 mm/year (Figure 7).
Results from the potentiostatic tests (Figure 7) suggest that the crevice corrosion potential for Alloy 22 in 5 M $CaCl_2$ at 120°C is between –100 mV and –150 mV SSC. Comparing these results with the crevice repassivation potentials in Table 2 and Figure 6, it seems apparent that the crevice repassivation potentials obtained through CPP (ER1 or ERCO) are too conservative for these tested conditions, that it, in the most aggressive higher temperature range, the repassivation potentials obtained using the THE test (ER,CREV) may represent better the behavior of the alloy.



**Effect of Chloride Concentration**

Cyclic Potentiodynamic Polarizations (CPP)

Figure 9 shows the cyclic potentiodynamic polarization for a MA Alloy 22 specimen in deaerated 0.5 M and 0.0005 M NaCl at 90°C. In both solutions the passive current density was between 0.1 and 1 μA/cm². The breakdown potential (E20) was higher in the 0.0005 M solution (650 mV SSC) than in the 0.5 M solution (430 mV SSC). The specimen tested in the more dilute solution was polarized to exceedingly high potentials of near 2 V SSC. The vertical shape of the final anodic portion of the polarization curve is a consequence of the low conductivity of the electrolyte, which did not allow for the applied current to reach the working electrode. In the reverse scan, the current approximately traced the path for the forward scan, suggesting the absence of localized corrosion (crevice corrosion). After the test, the specimen tested in the 0.0005 M NaCl solution suffered substantial transpassive dissolution in the boldly exposed surfaces and negligible shallow grain boundary or interdendritic etching in the creviced areas (Figure 10). The boldly exposed surfaces were yellow and the weld appeared etched due to the forced current applied for long testing time. In the 0.5 M NaCl solution, the polarization curve showed a delayed hysteresis in the reverse scan suggesting the presence of crevice corrosion. The specimen tested in the 0.5 M NaCl solution was also yellow and suffered transpassive dissolution in the boldly exposed surfaces as a consequence of the high applied potential of almost 1 V SSC. Besides the transpassive dissolution, the specimen tested in the 0.5 M NaCl solution also suffered crevice corrosion at discrete spots under the crevice formers (Figure 11).

Comparison Between CPP and THE

Figure 12 shows individual values of the repassivation potentials ER1 and ERCO from CPP tests for Alloy 22 as a function of the chloride concentration at 90°C. The values of repassivation potentials for MA Alloy 22 specimens in 4 M NaCl are from Reference 21. The lines represent average values of ER1 and ERCO for both ASW and MA specimens since there were no practical differences between the repassivation potentials of welded and non-welded specimens. Also, there are no practical differences between ER1 and ERCO. Figure 12 shows that in general, the repassivation potential (ER) decreased as the chloride concentration increased according to the equation

$$ER = A - B \cdot \log[Cl^-] \qquad (1)$$

where A and B are constants that depend on the temperature. The same relationship between repassivation potential and chloride concentration has been reported before for Alloy 22 by Brossia et al. [22].

Figure 13 shows the repassivation potentials (ER,CREV) obtained using the THE method. The ER1 line fit from Figure 12 is also included. ER,CREV shows the same relationship with the chloride concentration as ER1 did, and the slopes (fits) are almost parallel. Figure 14 shows comparatively the same data from Figure 13 plus the addition of previously published data by other researchers [22]. The values currently reported seem more reproducible (Figures 12-13) and show a lower boundary for the repassivation potential, i.e. more conservative, than the published data [22]. The discrepancy in the two sets of data could be related to the different nature and geometry (tightness) of the crevice former devices used in both sets of data.



## CONCLUSIONS

1. The susceptibility of Alloy 22 to crevice corrosion markedly varied with the temperature and chloride concentration in the electrolyte. The higher the temperature and the chloride concentration the lower the resistance to crevice corrosion.

2. The susceptibility of Alloy 22 to crevice corrosion can be assessed using the crevice repassivation potential as a parameter. This repassivation potential was called ER1 using cyclic potentiodynamic polarization (CPP) curves and ER,CREV using the Tsujikawa-Hisamatsu Electrochemical (THE) method.

3. In general, there was excellent agreement between the repassivation potential using both methods (CPP and THE).

4. In less aggressive conditions (lower temperatures and chloride concentration) the THE method gave lower repassivation potentials than the CPP method.

5. In more aggressive conditions (higher temperatures and chloride concentration) the CPP method gave lower repassivation potentials than the THE method.

6. Potentiostatic tests showed that in aggressive conditions the repassivation potential measured using the CPP method is conservative.

7. When crevice corrosion occurred on the tested specimen, the weld seam was not more susceptible to attack than the base metal.

## ACKNOWLEDGMENTS

This work was performed under the auspices of the U. S. Department of Energy by the University of California Lawrence Livermore National Laboratory under contract N° W-7405-Eng-48. The work was supported by the Yucca Mountain Project, which is part of the DOE Office of Civilian Radioactive Waste Management (OCRWM).

## REFERENCES

1. ASTM International, Volume 03.02, Standards G 5, G 15, G 48, G 59, G 61, G 102 (ASTM International, 2003: West Conshohocken, PA).
2. Haynes International, "Hastelloy C-22 Alloy", Brochure H-2019E (Haynes International, 1997: Kokomo, IN).
3. R. B. Rebak in Corrosion and Environmental Degradation, Volume II, p. 69, Wiley-VCH, Weinheim, Germany (2000).
4. R. B. Rebak and P. Crook, *Advanced Materials and Processes*, February 2000.
5. Yucca Mountain Science and Engineering Report, U. S. Department of Energy, Office of Civilian Radioactive Waste Management, DOE/RW-0539, Las Vegas, NV, May 2001.
6. G. M. Gordon, Corrosion, 58, 811 (2002).
7. B. A. Kehler, G. O. Ilevbare and J. R. Scully, Corrosion, 1042 (2001).
8. K. J. Evans and R. B. Rebak in Corrosion Science – A Retrospective and Current Status in Honor of Robert P. Frankenthal, PV 2002-13, p. 344-354 (The Electrochemical Society, 2002: Pennington, NJ).
9. K. J. Evans, S. D. Day, G. O. Ilevbare, M. T. Whalen, K. J. King, G. A. Hust, L. L. Wong, J. C. Estill and R. B. Rebak, PVP-Vol. 467, Transportation, Storage and Disposal of Radioactive Materials – 2003, p. 55 (ASME, 2003: New York, NY).
10. S. D. Day, K. J. Evans and G. O. Ilevbare, in "Critical Factors in Localized Corrosion IV", PV 2002-24, p. 534 (The Electrochemical Society, 2003: Pennington, NJ).
11. D. S. Dunn, G. A. Cragnolino, and N. Sridhar, in Scientific Basis for Nuclear Waste Management XXIV, Vol. 608, p 89 (Materials Research Society, 2000: Warrendale, PA).
12. G. A. Cragnolino, D. S. Dunn and Y.-M. Pan, in Scientific Basis for Nuclear Waste Management XXV, Vol. 713, p 53 (Materials Research Society, 2002: Warrendale, PA).
13. V. Jain, D. Dunn, N. Sridhar and L. Yang, Corrosion/2003, Paper 03690 (NACE International, 2003: Houston, TX).
14. D. S. Dunn, L. Yang, Y. – M. Pan and G. A. Cragnolino, Corrosion/2003, Paper 03697 (NACE International, 2003: Houston, TX).



15. N. S. Meck, P. Crook, S. D. Day and R. B. Rebak, Corrosion/2003, Paper 03682 (NACE International, 2003: Houston, TX).
16. J. H. Lee, T. S. E. Summers and R. B. Rebak, Corrosion/2004, Paper 04692 (NACE International, 2004: Houston, TX).
17. D. S. Dunn, G. A. Cragnolino, Y. M. Pan and L. T. Yang, Corrosion/2004, Paper 04698 (NACE International, 2004: Houston, TX).
18. S. Tsujikawa and Y. Hisamatsu, Corr. Eng. Japan, 29, 37 (1980).
19. M. Akashi, G. Nakayama and T. Fukuda, Corrosion/98, Paper 98158 (NACE International, 1998: Houston, TX).
20. K. J. Evans, L. L. Wong and R. B. Rebak "Determination of the Crevice Repassivation Potential of Alloy 22 by a Potentiodynamic-Galvanostatic-Potentiostatic Method," PVP-ASME Vol. 483, pp. 137-149 (American Society of Mechanical Engineers, 2004: New York, NY).
21. G. O. Ilevbare, "The Effect of Sulfate Anions on the Crevice Corrosion in Alloy 22" (Submitted for publication to Corrosion Journal).
22. C. S. Brossia, L. Browning, D. S. Dunn, O. C. Moghissi, O. Pensado and L. Yang "Effect of Environment on the Corrosion of Waste Package and Drip Shield Materials," Publication of the Center for Nuclear Waste Regulatory Analyses (CNWRA 2001-03), September 2001.
23.

Table 1
Chemical Composition in Weight percent of the Materials Used for Testing

| Element | Ni | Cr | Mo | W | Fe | Others |
|---|---|---|---|---|---|---|
| Nominal ASTM B 575 | 50-62 | 20-22.5 | 12.5-14.5 | 2.5-3.5 | 2-6 | 2.5Co-0.5Mn-0.35V max. |
| Type of Specimen/Heat | | | | | | |
| SRG04, Base (MA) Heat 059902LL1 | 59.56 | 20.38 | 13.82 | 2.64 | 2.85 | 0.17V-0.16Mn |
| DEA Base (MA) Heat 2277-1-3265 | ~57 | 21.2 | 12.9 | 2.5-3.5 | 3.9 | 0.7Co-0.25Mn-0.17V |
| JE1601-1700 Base Heat 0599902LL1 | 59.56 | 20.38 | 13.82 | 2.64 | 2.85 | 0.17V-0.16Mn |
| JE1618-1651and JE1671-1700 Weld Wire Heat XX1829BG | 59.31 | 20.44 | 14.16 | 3.07 | 2.2 | 0.21Mn-0.15Cu |
| JE1601-1617 and JE1652-1670 Weld Wire Heat XX1753BG | 59.7 | 20.54 | 14 | 3.1 | 2.08 | 0.2 Mn |
| KE0101-0150 Base Heat 059902LL2 | 59.56 | 20.38 | 13.82 | 2.64 | 2.85 | 0.16Mn-0.17V |
| KE0101-0150 Weld Wire Heat XX2048BG | 59.4 | 20.48 | 14.21 | 3.02 | 2.53 | 0.2Mn |
| KE0151-0239 Base Heat 2277-0-3183 | 55.29 | 21.23 | 13.37 | 2.93 | 3.65 | 1.7Co-0.23Mn-0.14V |
| KE0151-0239 Weld Wire Heat XX1829BG | 59.31 | 20.44 | 14.16 | 3.07 | 2.2 | 0.21Mn-0.15Cu |

Table 2: Average Repassivation Potentials for Alloy 22 in 5 M $CaCl_2$ in mV SSC as a function of temperature using both CPP and THE. (*) Denotes a single value.

| Temperature (°C) | Average ER1 (MA) CPP | Average ERCO (MA) CPP | Average ER1 (ASW) CPP | Average ERCO (ASW) CPP | Average ER, CREV (ASW) THE |
|---|---|---|---|---|---|
| 30 | NA | NA | 692 | NA | -4 * |
| 45 | 455 | 539 | 348 | 218 | -44 * |
| 60 | 288 | -7 | -86 | -60 | -60 |
| 75 | -110 | -94 | -125 | -136 | NA |
| 90 | -182 | -121 | -175 | -174 | -130 |
| 105 | -192 | -195 | NA | NA | -127 * |
| 120 | -199 | -190 | -215 | -155 | -136 |
| | | | | | |

NA = Not Available or Not Applicable, CPP = Cyclic Potentiodynamic Polarization, THE = Tsujikawa Hisamatsu Electrochemical



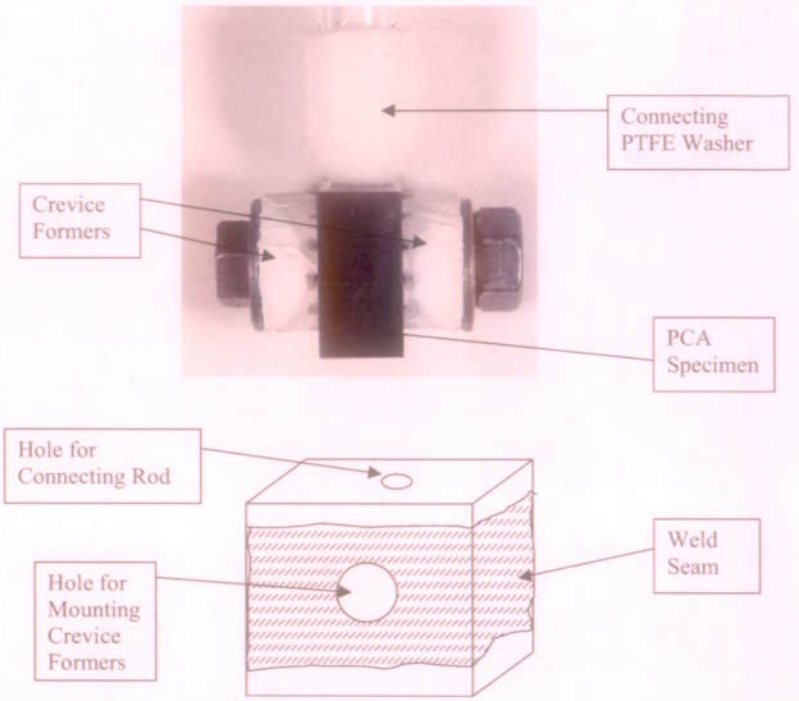


Figure 1: PCA Specimen (0.75 x 0.75 x 0.375 inch or approx. 20 x 20 x 10 mm),

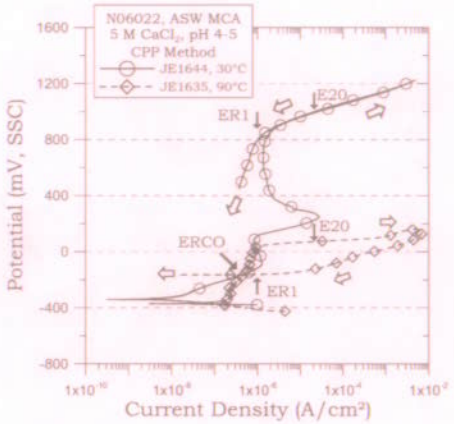


Figure 2: CPP for Alloy 22 in 5 M $CaCl_2$ brines.

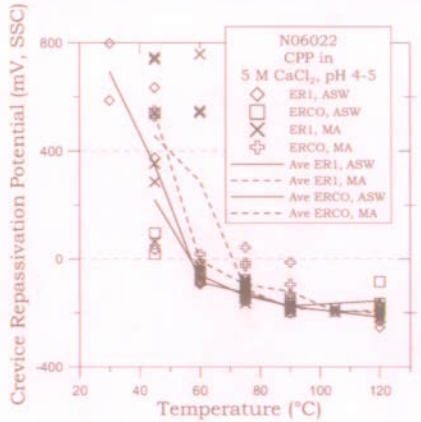


Figure 3: Repassivation Potentials (ER1 and ERCO) for Alloy 22 in 5 M $CaCl_2$.



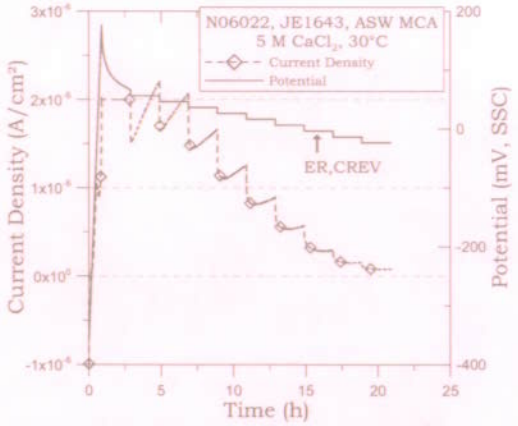


Figure 4: THE test of Alloy 22 in 5 M $CaCl_2$ at 30°C.

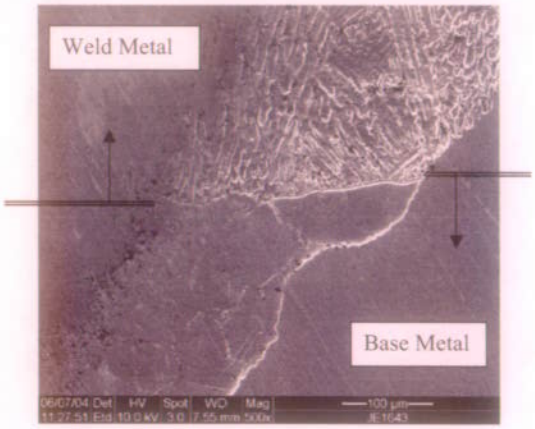


Figure 5: SEM image of the crevice corrosion in specimen JE1643. Tested using THE in 5 M $CaCl_2$ at 30°C. Mag. X 500.

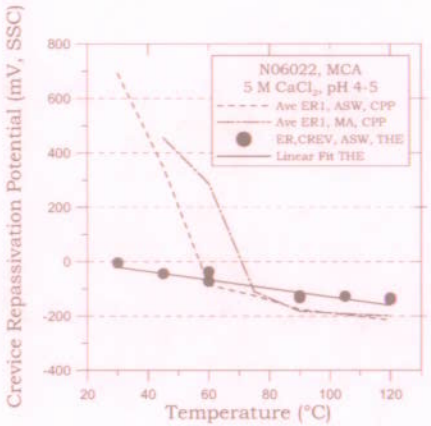


Figure 6: Comparison Between ER1 and ER,CREV for Alloy 22 in 5 M $CaCl_2$

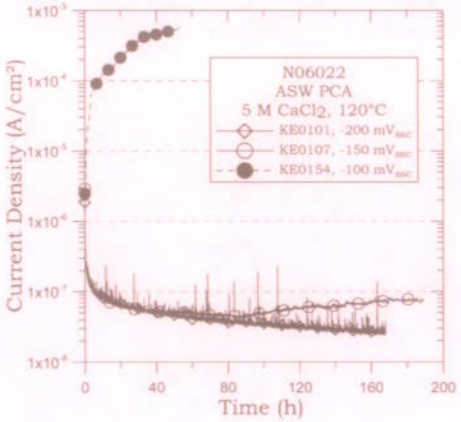


Figure 7: Potentiostatic tests of Alloy 22 in 5 M $CaCl_2$ at 120°C.



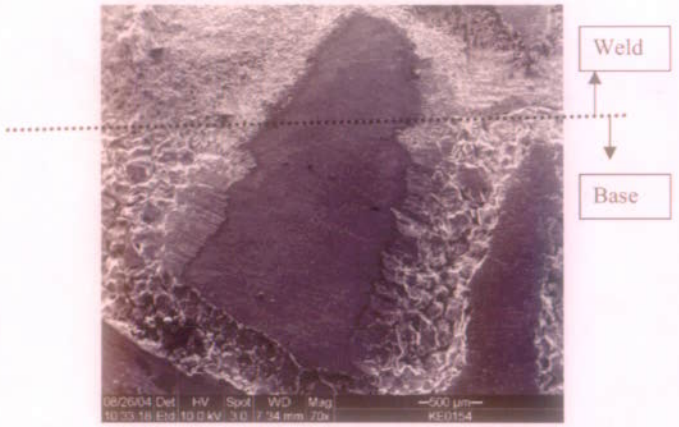


Figure 8: Localized Corrosion in Alloy 22 polarized to –100 mV SSC in 5 M $CaCl_2$ at 120°C (Fig. 7). Mag. X 70.

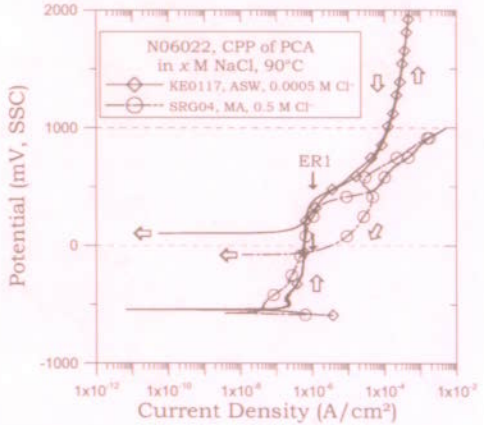


Figure 9: CPP for Alloy 22 in 0.5 M and 0.0005 M NaCl at 90°C.

Figure 10: Interdendritic etching in the creviced area of Alloy 22 tested in 0.0005 M NaCl at 90°C. Mag. X 1000.

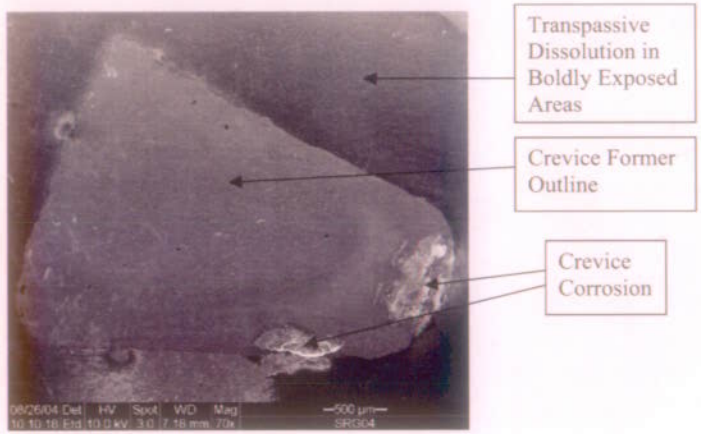


Figure 11: Crevice corrosion of Alloy 22 tested in 0.5 M NaCl at 90°C. Mag. X 70.



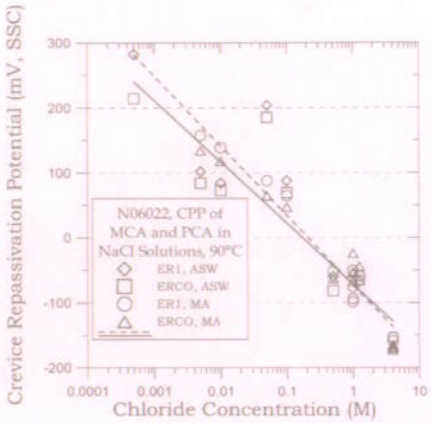


Figure 12: Repassivation Potential for Alloy 22 using CPP in NaCl Solutions.

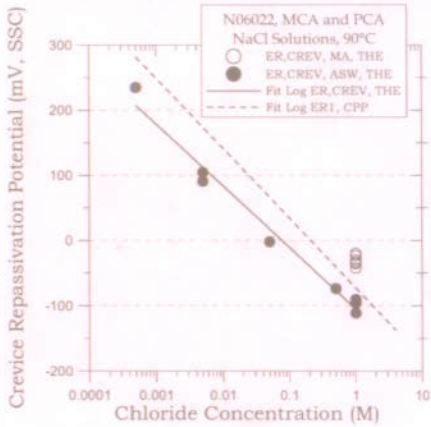


Figure 13: Comparison of the Repassivation Potential using CPP and THE.

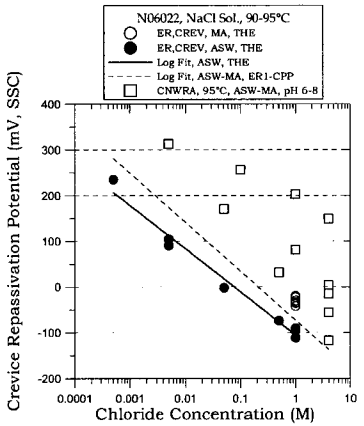


Figure 14: Comparison of the Repassivation Potential using current data with published data from another laboratory.